Talanta 311 (2027) 130255

Contents lists available at ScienceDirect

Talanta

journal homepage: www.elsevier.com/locate/talanta

Electrochemical determination of Azelastine using a Calix[4]arene-doped polyaniline screen-printed sensor in pharmaceutical and biological samples

Rawan S. El Meniawy [a,b], Sarah S. Saleh [b], Yasmin Rostom [c], Mona T. Ragab [c,*]

[a] Postgraduate program, in Pharmaceutical Analytical Chemistry, Faculty of Pharmacy, Cairo University, Kasr El-Aini St., Cairo, ET-11562, Egypt
[b] Analytical Chemistry Department, Faculty of Pharmacy, October University for Modern Sciences and Arts (MSA), 6th of October City, 11787, Egypt
[c] Pharmaceutical Analytical Chemistry Department, Faculty of Pharmacy, Cairo University, Kasr El-Aini St., Cairo, ET-11562, Egypt

ARTICLE INFO

Keywords:
Aqueous humor
Azelastine
AGREE
Calix[4]arene
NQS
Polyaniline
Screen-printed electrode

ABSTRACT

Careful choice of ion-sensing components and substrates is the primary focus when developing ion-selective electrodes to achieve maximum sensitivity, selectivity, stability and accuracy. This study aims to develop and optimize two miniaturized screen-printed solid-contact ion-selective electrodes to quantify Azelastine HCl (AZE) in various pharmaceutical preparations and complex spiked biological samples. The electrodes' optimization involved doping ion-sensing membranes with the most selective ionophore for the studied drug, followed by electro-polymerization of polyaniline (PANI) conducting polymer at screen-printed electrode. Two screen-printed electrodes were developed for AZE determination, and their electrochemical performance was evaluated following IUPAC recommendations. The optimal calix[4]arene-doped PANI-based screen-printed electrode reached a detection limit of 2.50×10^{-6} M for AZE with a dynamic response of about 3 s. It successfully quantified AZE in its pure form, pharmaceutical dosage forms, spiked aqueous humor and plasma, which demonstrates potential applicability. Its selectivity was assessed in the presence of the induced degradation products of AZE, interfering ions, and the co-formulated drug, fluticasone propionate. A comparison regarding greenness between the developed and two reported methods was established by means of Modified Green Analytical Procedure Index (Mo-GAPI) and Analytical Greenness (AGREE) assessment tools. Sustainability profile was established using NQS index, showing alignment of the study with the UN-17 SDGs.

1. Introduction

Analysis techniques based on potentiometry can be titled as one of the most crucial techniques used in the electrochemistry field [1]. Ion-selective electrode (ISE) is an analytical instrument that quantifies ionic activity in aqueous solutions through detection of electrical potential correlating directly with analyte concentration [2]. ISE is commonly used for its many advantages compared to other analytical techniques, such as its easy and affordable operation, accuracy, eco-friendliness and relatively being of low cost [3]. The earliest ISEs were the conventional liquid-contact (LC) ones based on internal solutions [4]. They had many disadvantages such as evaporation and permeation of internal solutions, short life span, and unsteady response. To satisfy the need for analytical ion-selective electrodes that offer stable and reproducible responses as well as easy control and long-term preservation, solid-contact ion-selective electrodes (SC-ISEs) were introduced [3].

SC-ISEs represent the latest stage of potentiometric electrodes for ion detection. They provide advantages over liquid-contact sensors, such as miniaturization, on-site disposable analyzers, rapid response, versatility, relatively low production cost, ease of application, uniform surface integration, portability, robust stability and improved detection in complex matrices [5]. Moreover, SC-ISEs polymeric ion sensing membranes (ISM) are simpler to be compatible, more flexible with modern 3D printing, and can be miniaturized [6]. A couple of examples for SC-ISEs are the metallic carbon or glassy ones [7], classical coated wire electrodes [8], microfabricated copper electrodes [9] and recently screen-printed electrodes (SPEs) [10]. Some significant obstacles occurred upon using SC-ISEs such as developing internal liquid films between ISM and solid substrate, a rise in potential effect upon contact with some aqueous solutions, sudden changes occurring in the screen printed substrates composition [11], and its high sensitivity towards oxygen, light, pH, and CO_2 [12]. Using hydrophobic ion-to-electron transducers as high redox capacitance conducting polymers can

* Corresponding author.
E-mail address: mona.abdelhafez@pharma.cu.edu.eg (M.T. Ragab).

https://doi.org/10.1016/j.talanta.2026.130255
Received 3 November 2025; Received in revised form 8 June 2026; Accepted 1 July 2026
Available online 2 July 2026

overcome the previous drawbacks. The inclusion of such conducting polymers results in significant improvements in potential drifts and detection limits [13].

A widely applicable recent approach in SC-ISEs is the incorporation of hydrophobic redox mediator "polyaniline" (PANI) as an ion-to-electron conducting polymer [14]. It has been reported that PANI increased the electrical signal stability owing to its hydrophobic nature that blocks creation of water at the electrode/ion sensing membrane boundary. Additionally, rapid ion-to-electron transduction enables an obvious fast response [15]. Polyaniline polymerization can be carried out electrochemically or chemically [16]. Electrochemical polymerization possesses numerous benefits, such as being applicable at room temperature and omitting the need for any free radical initiators, oxidants, or sources of radiation. Moreover, electro-polymerization parameters, potential, current density, and number of cycles are controllable, resulting in manageable film thickness and porosity [15]. It has been reported that ionophores, molecular recognition compounds, can be doped into ion-sensing membranes to increase the sensitivity and selectivity of ISEs [17]. Thus, combining the benefits of SC-ISEs with those of ionophores and ion-to-electron transducers, such as PANI, can result in fabrication of miniaturized, eco-friendly, portable, highly stable, selective and sensitive SC-ISEs.

Azelastine HCl (AZE); 4-[(4-chlorophenyl) methyl]-2-(hexahydro-1-methyl-1H-azepin-4-yl)-, mono-hydrogen chloride (Fig. S1) [18]. It has been specified as the first medication for treating allergic and non-allergic rhinitis according to World Health Organization and the American Academy of Allergy [19]. It is a medication that is available in the form of ophthalmic drops to treat allergic conjunctivitis and in the form of intranasal spray that is used to treat allergic symptoms caused by seasonal allergic rhinitis or perennial allergic rhinitis or any upper respiratory allergies. Various analytical methods have been reported for determining AZE either in its pure form or in dosage forms, such as spectrophotometric methods [20–22], spectrofluorimetric methods [23,24], electrochemical methods [25–28], HPLC [29–31], TLC [32], and LC/MS/MS [33,34].

With respect to the literature at hand, no research has been published that combines the use of an environmentally friendly, miniaturized, portable, selective, accurate, and stable analytical tool. Thus, the aim of this study is to determine AZE in its pure powdered form, ophthalmic solution, nasal spray, and in different spiked biological samples, rabbit aqueous humor, and human plasma. A key challenge for our method is the determination of azelastine in different spiked biological matrices that demonstrate potential applicability. Analysis in plasma is important because 40% of an intranasal dose of AZE reaches the systemic circulation [35]. Rabbit aqueous humor was chosen due to azelastine's use in ophthalmic formulations for allergic conjunctivitis [36], with rabbits serving as the standard model for ocular pharmacokinetic studies. In addition, AZE will be analyzed without interference from its possible degradation products and related active and inactive ingredients using an optimized, highly selective, eco-friendly, miniaturized, portable screen-printed electrode (SPE). Moreover, we aim to perform this work using the optimized electrode with no need for any pretreatment or extraction procedures for the analyzed samples.

Evaluating and validating the results obtained by both SPEs according to ICH guidelines [37] and IUPAC recommendations [38] clarified how PANI inclusion improved the electrode's sensitivity. Ultimately, the environmental impact of the developed method and two previously published approaches for AZE determination has been compared regarding their greenness profiles using AGREE assessment tool [39] and Mo-GAPI one [40]. The sustainability profile of the method using NQS index showed alignment of the study with the UN-17 SDGs.

2. Experimental

2.1. Instruments

Jenway 3510 digital ion analyzer (Essex, UK) was provided with a double-junction Ag/AgCl reference electrode (Thermo Scientific Orion 900200, USA; inner filling solution; 3.0 M KCl saturated with AgCl. Salt bridge electrolyte; 10% KNO_3) were used for potentiometric measurements. Jenway pH glass electrode no. 924005-BO3-Q11C (Essex, UK) was used for pH measurements. Metrohm Autolab PGSTAT204 potentiostat/galvanostat from Netherlands, running Nova 1.11 software, was employed for the electro-polymerization process, cyclic voltammetry and electrochemical impedance spectroscopy measurements. The morphology of the deposited PANI was examined via scanning electron microscope (SEM, model S-4700, Hitachi, Japan) and high-resolution transmission electron microscope (HRTEM, JEM 2100 HRT, Japan). Bandelin Sonorex magnetic stirrer, Rx510S (Budapest, Hungary), was utilized to stir samples continuously. An oven was used to dry.

2.2. Materials and reagents

Pure AZE was obtained from Hikma Pharma (batch number WS/AZEL-BP/22.1), with a purity of 99.51% ± 0.76 as determined by the official British Pharmacopoeia direct potentiometric titration procedure [18]. Pure samples of fluticasone propionate and ipratropium bromide were provided by Hikma Pharma and NODCAR, respectively. Zelagap® ophthalmic solution, (B.N. 24025004) marked to hold 0.5 mg of Azelastine HCl per 1 mL, was acquired from a local pharmacy in Cairo, Egypt. It is manufactured by Global Advanced Pharmaceuticals (GAP), Cairo, Egypt. Azelast Plus® nasal spray suspension (B.N. I244) was also purchased from a local pharmacy in Cairo, Egypt. It is marked to hold 0.137 mg of Azelastine HCl per unit dose. It is manufactured by Hikma Pharma, Giza, Egypt. Aniline, high molecular weight Polyvinyl chloride (PVC), potassium tetrakis(4-chlorophenyl)borate (K-TCPB), calix[4]arene (CX4), calix[6]arene (CX6), 4-tertbutylcalix[8]arene (t-Bu-CX8), orthophosphoric acid solution, and sodium phosphate monobasic were supplied by Sigma-Aldrich, Steinheim, Germany. 2-nitrophenyl octyl ether (*o*-NPOE) was purchased from Alfa Aesar (Karlsruhe, Germany). Tetrahydrofuran was obtained from Fisher Scientific, Loughborough, UK. Merck/Darmstadt, Germany supplied us with Tetrabutylammonium hydrogen sulfate (TBAHS). Carbon screen-printed electrodes (3 mm diameter) were obtained from CH Instruments, Inc. (TX, USA). Potassium chloride, sodium hydroxide, magnesium chloride, calcium chloride, concentrated sulphuric acid, and concentrated hydrochloric acid were acquired from El-Nasr Pharmaceutical Chemical Company, Cairo, Egypt. A phosphate buffer of pH 3.0 was formulated by dissolving 2.4 g of sodium phosphate monobasic in 700 mL of water. Then, adjusting the pH to 3.0 was done by using 10% v/v orthophosphoric acid solution, and the volume was completed with water to 1000 mL. All the previous chemicals used were of analytical grade, and bi-distilled water was used in all preparations. Rabbit aqueous humor was obtained from the animal house of Faculty of Pharmacy, Cairo University, and the collected samples were maintained at −2°C in storage until they were needed for use. Human plasma was purchased from VACSERA, Egypt.

2.3. Stock, working solutions & spiked biological samples

2.3.1. Azelastine HCl (AZE) solutions

A 1.00×10^{-2} M stock standard solution of Azelastine HCl was formulated by dissolving 0.1046 g in phosphate buffer at pH 3.0 and bringing to final volume in a 25-mL volumetric flask. The volume was then made up to the mark using the same buffer. AZE working solutions were established by serially diluting the stock standard solution with phosphate buffer pH 3.0 to obtain solutions in the concentration range of 1.00×10^{-7} to 1.00×10^{-3} M.

2.3.2. Azelastine HCl (AZE) degradation product solutions (acidic/alkaline/oxidative)

Acidic, Alkaline, & Oxidative degradation products of AZE were conducted according to the reported method [30], by transferring aliquots of AZE solution into screw-capped glass vials, followed by 1 M HCl, 0.5 M NaOH, and 9% w/v H_2O_2. Then, for acidic and oxidative degradation products, heat in a thermostatically controlled water bath at 80^0C and for the alkaline at 60^0C, both for 60 min. After the specified duration, samples were cooled, and those subjected to acidic or alkaline conditions were brought to neutral pH. The resulting solutions were transferred to a set of 10-mL volumetric flasks to obtain a concentration of 2.4×10^{-4} M for each solution.

2.4. Procedures

2.4.1. Electrochemical grafting of polyaniline (PANI) onto screen-printed electrode (SPE) surface (modified SPE/PANI electrode)

Electro-polymerization was performed via cyclic voltammetry using a potentiostat/galvanostat instrument aided by Nova 1.11 software. Electrochemical polymerization of PANI onto SPE working electrode was accomplished from 0.1 M aniline in 0.1 M H_2SO_4 vs. Ag/AgCl reference electrode and Pt counter electrode. Cyclic voltammetric parameters were chosen as per previously published work [15] with modification in the number of cycles. The scan was carried out in the range from −0.1 to 1.0 V vs. Ag/AgCl reference electrode at 0.05 V/s scan rate [15]. The cycle number was set at 40 cycles to ensure a thick, uniform polymer coating on the SPE surface [41].

2.4.2. Morphological and surface characterization of PANI film

Morphological features of the deposited PANI were characterized by scanning electron microscopy (SEM) of the modified SPE/PANI electrode. To complement the SEM findings, high-resolution transmission electron microscopy (HRTEM) and HRTEM-selected area electron diffraction (SAED) have been employed by extracting the PANI film using 2 drops of ethanol followed by sonicating the obtained suspension for 15 min, then loaded on carbon-coated copper grid and left to dry before examination.

2.4.3. Electrochemical characterization of SPE/PANI

The electrochemical performance of the modified SPE/PANI electrode was examined using a 10 mM $[Fe(CN)_6]^{3-}/[Fe(CN)_6]^{4-}$(1:1) redox probe in 0.1 M KCl as the supporting electrolyte. To measure the active surface area of the modified SPE/PANI electrode, cyclic voltammetry (CV) was carried out within the potential window of 0.0–1.2 V (vs. Ag/AgCl) at a scan rate of 40 mV/s. Electrochemical impedance spectroscopy (EIS) was performed in a conventional three-electrode setup over the frequency range of 0.1 Hz to 100 kHz using same solution as the redox probe [42]. Fitting of the obtained spectra to a Randles equivalent circuit was achieved using NOVA software (version 1.11) to estimate the corresponding circuit parameters.

2.4.4. Ion-sensing membranes fabrication and electrodes assembly

Three ionophore-doped ion sensing membranes (ISMs) were prepared by dissolving 190.0 mg PVC, 1.4 mg K-TCPB, 0.4 mL *o*-NPOE and 3.8 mg of the tested ionophore in about 6.0 mL THF. The doped ionophores were CX4, CX6 and CX8. Then into 3 Petri dishes of 5 cm diameter, the three prepared solutions were poured, afterwards dishes were covered with three filter papers allowing THF to evaporate overnight at room temperature. Three ion-sensing membranes (ISMs) with a thickness of ~0.1 mm were obtained which were then used for the liquid contact (LC) sensors, LC/CX4, LC/CX6 and LC/CX8 assembly. From each ISM a disc of about 8 mm diameter was cut and adhered with THF to a transposable PVC tip of its respective electrode. An internal reference solution of 1.00×10^{-3} M AZE and KCl prepared in phosphate buffer, pH 3.0 was used. Ag/AgCl wire (1-mm diameter) was dipped in the internal reference solution to function as an internal reference electrode. The first screen-printed electrode (SPE/PANI/CX4 electrode) was assembled by drop-casting 20.0 μL of the CX4-doped ISM, before THF evaporation, onto a screen-printed electrode (SPE) modified with PANI as explained under ***2.4.1*** and then left to dry at room temperature overnight. The second screen-printed electrode (SPE/CX4 electrode) was prepared as SPE/PANI/CX4 but onto SPE lacking PANI layer. The fabricated electrodes, LC/CX4, LC/CX6, LC/CX8, SPE/PANI/CX4, and SPE/CX4 were conditioned by soaking in a 1.00×10^{-3} M AZE. Composition of the five fabricated ion-selective electrodes is illustrated in Table 1.

2.4.5. Degree of selectivity of ionophore-doped membranes

The potential difference (ΔE) is equal to (E_i - E_{TBAHS}) in emf values of the three liquid-contact sensors with ionophore-doped membranes (LC/CX4, LC/CX6, and LC/CX8 sensors) in response to 1.00×10^{-3} M AZE and 1.00×10^{-3} M TBAHS were recorded.

2.4.6. Screen-printed electrodes' calibration

Double junction Ag/AgCl external reference electrode was separately conjugated with each electrode, SPE/PANI/CX4 and SPE/CX4 electrodes, along with a Jenway digital ion analyzer to carry out the potentiometric measurements. Serial dilutions of AZE ($1.00x10^{-7}$ – $1.00x10^{-2}$ M) using phosphate buffer pH 3.0 were prepared. The assembled electrodes were immersed in stirred AZE solutions in conjugation with the reference electrode then the potentiometer recorded electromotive force (*emf*) of each solution. A calibration curve was established for each electrode by plotting changes in *emf* against - log molar concentrations of AZE and the respective regression equation was computed.

2.4.7. Screen-printed electrodes' validation by IUPAC

Validity of two SPEs was examined according to IUPAC guidelines [38] for linearity and range, accuracy, precision, and limit of detection (LOD).

2.4.8. Water layer and signal drift tests on screen-printed electrodes

To assess the impact of PANI on performance and stability of SC-ISEs, water layer and signal drift tests were performed on the fabricated SPEs (SPE/PANI/CX4 and SPE/CX4). The potential response of $1.00x10^{-3}$ M AZE solution was recorded by the two electrodes for 1 h. Then the two electrodes were immersed in $1.00x10^{-2}$ M ipratropium bromide solution and their potential responses were recorded for another hour. Finally, the two electrodes were immersed back into the $1.00x10^{-3}$ M AZE solution for the last (third) hour and the obtained potential values were recorded. The signal drift was monitored for the two SPEs by documenting *emf* readings every 2 min for the first hour.

2.4.9. Applications of SPE/PANI/CX4 electrode

a. Potentiometric determination of Azelastine HCl in Zelagap® ophthalmic solution

Into two 25-mL volumetric flasks, aliquots of 2.09 mL and 209 μL were transferred from Zelagap® ophthalmic solution. To another two 25-mL volumetric flasks, aliquots of 15.9 mL and 1.59 mL were added. The contents of the two volumetric flasks were brought to the indicated volume using phosphate buffer (pH 3.0). Concentrations of the two resulting solutions were stated to be 1.00×10^{-4} and 1.00×10^{-5} AZE, respectively. Potential measurements of the prepared solutions were conducted using SPE/PANI/CX4 electrode paired with a double-junction Ag/AgCl reference electrode. Concentrations were calculated by applying the regression equation derived from the electrode.

b. Potentiometric determination of Azelastine HCl in Azelast Plus® nasal spray suspension

After thoroughly shaking the Azelast Plus® nasal spray suspension,

Table 1
Composition of the five fabricated ion-selective sensors.

No. of sensor	Sensor name	Nature of sensor	Polymeric matrix	Plasticizer	Ionophore	Cationic exchanger	Ion-to-electron transducer
1	LC/CX4	Liquid-contact electrode	PVC	*o*-NPOE	CX4	K-TCPB	-
2	LC/CX6				CX6		-
3	LC/CX8				CX8		-
4	SPE/PANI/CX4	Screen- printed electrode			CX4		PANI
5	SPE/CX4				CX4		-

aliquots of 15.9 mL and 1.59 mL were added to two 25-mL volumetric flasks, and volumes were completed to the mark using phosphate buffer pH 3.0. It was claimed that the final mixtures had concentrations of 1.00×10^{-3} M and 1.00×10^{-4} M AZE, respectively. SPE/PANI/CX4 electrode and the double-junction Ag/AgCl reference electrode were used to measure potential values of the produced mixtures. The electrode's associated regression equation was used to determine the corresponding concentrations.

c. Potentiometric determination of Azelastine HCl in spiked biological samples (rabbit aqueous humor and human plasma)

AZE concentrations of $1.00x10^{-3}$ M and $1.00x10^{-4}$ M in spiked rabbit aqueous humor and human plasma were obtained by adding 1 mL of $1.00x10^{-2}$ M and $1.00x10^{-3}$ M AZE working solutions, respectively, to 0.5 mL of each spiked biological samples into four separate 10-mL volumetric flasks and mixed by vortexing for 2 min. Then the volumes were made up to the mark using phosphate buffer pH 3.0. SPE/PANI/CX4 electrode and the double-junction Ag/AgCl reference electrode were used for recording potential values and subsequently the corresponding concentrations were computed.

2.4.10. Impact of interfering materials on SPE/PANI/CX4 electrode selectivity

The potential response of SPE/PANI/CX4 electrode towards certain interfering ions such as K^+, Na^+, Ca^{2+}, Mg^{2+}, Zn^{2+}, besides AZE acidic, alkaline and oxidative degradation products, and AZE co-formulated drug; fluticasone propionate was measured. The selectivity coefficients (Kpot) obtained are summarized in Table S1. Potentiometric selectivity coefficient, -log ($K^{pot}_{\text{primary ion interferent}}$), was calculated to investigate the extent of possible interference from these substances on the selectivity of the SPE/PANI/CX4 electrode towards AZE. For evaluating the selectivity coefficients, the separate solutions method (SSM) [43] was used by utilizing the following equation:

$$-log\left(K^{pot}_{primary\ ion\ interferent}\right) = \frac{E_I - E_{Drug}}{2.303RT/Z_{drug}F} + \left(1 + \frac{Z_{Drug}}{Z_I}\right) \log\,[drug]$$

E_{drug} and E_I represent potential readings recorded in a 1.00×10^{-3} M of drug and interferent ion solution, respectively. Symbol Z_{drug} and Z_I are the electrical charges of the drug and the interfering ion, respectively. while $2.303RT/Z_{drug}F$ corresponds to the slope of the tested electrode (measured in mV/decade).

All tested interfering substances showed selectivity coefficients (Kpot) below 1, indicating that the electrode has a lower affinity for these compounds than for AZE. Particularly low values were observed for fluticasone propionate and the acidic degradation product, indicating minimal interference under the experimental conditions. This selectivity can be explained by the distinct physicochemical characteristics of these substances relative to AZE. Fluticasone propionate is a relatively large, non-charged, and highly fat-soluble compound that lacks an easily protonatable group under the operating conditions, thereby limiting its electrostatic interactions with the electrode's active layer [44]. Likewise, the product formed during acid degradation is expected to exhibit altered structural and electronic properties that reduce its affinity for receptor sites. Selectivity toward AZE arises from its molecular structure and ionization state. At the working pH, AZE exists predominantly in a protonated cationic form due to its tertiary amine. This facilitates strong interaction with the CX4 ionophore via electrostatic attraction and non-covalent forces. The ionophore cavity accommodates the protonated AZE, enabling π–cation interactions with its aromatic rings and additional hydrophobic interactions, which collectively enhance molecular recognition. In contrast, inorganic cations such as Na^+, K^+, and Ca^{2+}, despite their charge, are characterized by high hydration energies and lack structural features that enable effective host–guest interactions within the hydrophobic cavity of CX4. This reduces their ability to compete with AZE at the binding sites, resulting in comparatively low interference.

2.4.11. Impact of pH and temperature on SPE/PANI/CX4 electrode function

Potential values of 1.00×10^{-3} and 1.00×10^{-4} M of AZE solution were measured at various pHs (2.0–8.5) to track the impact of pH on SPE/PANI/CX4 electrode performance. Potential values data that corresponded to different pH ranges were recorded. Additionally, electrode's potential values were recorded over a temperature range from 20°C to 30°C to investigate how temperature affects the electrode's performance.

3. Results and discussion

3.1. Ion-sensing membranes' composition

Ion sensing membranes (ISMs) consist of a PVC matrix that provides mechanical support and serves as a capture medium for ion association complexes. They are still demanding plasticization to dissolve the ion complex association with limitations on the choice of the mediators [45]. According to the quantity of the membrane components and the plasticizer type, the response and characteristics of PVC ISEs are drastically affected [46]. This adjustment helps in regulating the permittivity of the membrane by reaching the highest possible sensitivity and selectivity [47]. To reduce the membrane's electrical asymmetry along with protecting its parts from leaching into aqueous phase; optimizing proportion of plasticizer is a must [48]. Another main factor attributed to ISE fabrication and optimization is the type of ion exchanger used in the preparation of ISM. Ion exchangers can be defined as hydrophobic ionic sites that grant sensitivity to the membrane to exchange between the positively charged targeted ions and their cationic ions [49]. Also, in adjusting the selectivity and sensitivity towards the targeted ions or compounds by the ISE, a neutral molecule called an ionophore is added. This selective response is fundamentally based on molecular recognition, where the ionophore functions as a host for a target molecule acting as the guest [50]. The most popular class of supramolecular macrocycles studied nowadays is the calix[n]arenes. Calix[n]arenes are characterized as cavities that are basket-shaped and electron-rich and are mostly affected by their size influencing selectivity and binding strength to the intended ion through cation-π interactions [51].

In this present study, potassium tetrakis (4-chlorophenyl)borate (K-TCPB), which behaves as a cation exchanger, is added in the fabrication of AZE-ISMs. This choice was based on the fact that AZE has pKa value (strongest base) equal to 8.88 [52]; accordingly, it will act as a cation in the acidic medium. *o*-NPOE was selected as the plasticizer because of its high dielectric constant, which improves ion mobility and membrane

permeability [53]. Furthermore, to evaluate the effect of how the type of ionophore affects the selectivity of the sensing membranes, calix[n] arenes CX4, CX6, and CX8 were doped in the fabricated AZE-ISMs. It is worth noting that the pH conditions of the prepared working solutions played a fundamental role in achieving a complete ionization of AZE. Since AZE's pKa value equals 8.88, initial assessments were done using phosphate buffer of varied pH values (pH 3, 5, and 6). The selected pH was 3.0 as it enhanced the sensitivity towards AZE cationic microspecies by ten times compared to the other pH levels.

3.2. Degree of selectivity of ion-sensing membranes

The potentiometric approach can be used to determine both analyte ion concentration and the binding extent between a guest macromolecule and a host ion. Binding extent of organic ions can be determined through reference ion techniques, which have been reported in earlier studies [51], [54]. Therefore, the selectivity of the fabricated ionophore-containing ISMs toward AZE was assessed using TBAHS, which is a large hydrophobic ionic species. TBAHS acts as a reference ion that cannot attach to the ionophore cavities. Potential differences ($\Delta E = E_i - E_{TABHS}$) between emf values of the three liquid contact (LC)–ionophore-doped electrodes; LC/CX4, LC/CX6 and LC/CX8 in response to AZE, and TBAHS were computed. It was found that CX4-doped membrane (LC/CX4 electrode) had the lowest ΔE (99 mV) compared to ΔE of 210 mV with the CX6-doped membrane (LC/CX6 electrode) and 279 mV with the t-Bu-CX8-doped membrane (LC/CX8 electrode). These findings assured us that CX4 has the highest degree of selectivity for AZE. Subsequently, CX4-doped ISM has been drop-cast onto two screen-printed electrodes (SPEs).

3.3. Mechanism of interaction

Calixarenes are “basket-shaped” macrocycles capable of capturing drug molecules through selective host–guest interactions governed by cavity size, shape, and noncovalent force. Consequently, the optimal host for protonated AZE is determined not by calixarene size alone but by the compatibility of cavity dimensions and charge distribution with the guest molecule [55]. The preferential response toward AZE can be attributed to the better size complementarity between protonated AZE and the relatively small, rigid, and preorganized cavity of CX4. Calix[n] arenes show increasing cavity diameters with ring size, approximately 3.0, 7.6, and 11.7 Å for CX4, CX6, and CX8, respectively [56]. Although CX6 and CX8 possess larger cavities, their higher conformational flexibility may reduce selective recognition of AZE by decreasing host–guest complementarity. Therefore, CX4 is expected to provide a more defined microenvironment for AZE binding.

Computational analysis of the AZE–CX4 host–guest interaction showed an inclusion structure where AZE assumes a partially embedded configuration inside the CX4 cavity (Fig. S2). The formation of this complex is mainly facilitated by dispersion-based hydrophobic interactions between AZE's chlorophenyl group and the π-electron-abundant aromatic structures of CX4, occurring through π–π stacking mechanisms. Concurrently, the positively charged nitrogen atom in AZE's methylazepane section penetrates the CX4 cavity, positioning itself optimally for cation-π interactions with CX4's electron-rich aromatic rings, which additionally enhance complex stability. This binding configuration represents an equilibrium between energetically favorable non-covalent forces and spatial constraints within the restricted macrocyclic space. Together, these structural characteristics facilitate the creation of an energetically favorable supramolecular assembly and offer a molecular explanation for the experimentally detected changes in AZE's physicochemical properties following CX4 complexation, including possible influences on dissolution behavior, conformational stability, and molecular recognition capabilities. In summary, the enhanced selectivity demonstrated with CX4, relative to other evaluated macrocyclic ionophores, can be ascribed to superior compatibility between its cavity dimensions and the molecular size of protonated AZE (4-6 Å), combined with the synergistic effects of electrostatic and hydrophobic forces.

Building on this molecular recognition principle, the developed electrode exploits the selective capture of AZE in its protonated cationic form by CX4 as the recognition element. Upon recognition, AZE cations undergo an ion-exchange process with the ion exchanger, establishing a phase boundary potential at the membrane/solution interface. This potential is modulated by the activity of AZE ions in the aqueous phase and conforms to the Nernstian behavior characteristic of monovalent cation-selective electrodes.

3.4. Solid contact screen-printed electrode assembly

Long-term use of liquid-contact membrane electrodes does not demonstrate sufficient mechanical stability due to the limitations associated with the inner filling solution. This limitation inspired us to employ solid-contact miniaturized and portable screen-printed electrodes (SPEs) in our research using the most selective CX4-doped ISM. Also, we have studied the effect of the conducting polymer, PANI on the stability of SPEs via assembly of two SPEs. One SPE, namely SPE/PANI/CX4 electrode incorporated an electropolymerized PANI film via cyclic voltammetry at interface between electronically conducting solid substrate and CX4-doped ISM. A second electrode named SPE/CX4 was assembled using the CX4-doped ISM without incorporation of PANI layer.

The electro-polymerization of PANI is illustrated in Fig. 1. PANI's electro-polymerization was achieved from 0.1 M aniline as monomer in 0.1 M H_2SO_4 on the surface of SPE. The electro-polymerization process begins with the appearance of spiky anodic peaks around +0.8 V in the first three cycles of the initial anodic sweeps. Three anodic peaks with rising current are seen in each of the following cycles. Likewise, there are three equivalent broad reduction peaks in the cathodic sweep. The synthesis of radical cations (polaronic emeraldine) is responsible for the first peak at about +0.2 V; the formation of benzoquinone is responsible for the second peak around +0.5 V; and the formation of diradical dications is responsible for the third peak at 0.8 V. The autocatalytic character of the PANI electro-polymerization as reported in the literature [57], [58] is reflected in the fact that the current increases after each potential cycle, showing that the polyaniline film expands very quickly as the sweeping continues.

3.5. Morphological and surface characterization of PANI film

Scanning electron microscope (SEM) has been implemented as a quick, non-invasive, efficient, and potent tool that has been widely employed for imaging novel materials, particularly at the nano- and microscales [59]. As shown in Fig. 2, the SPE electrode modified with PANI film was examined using SEM, which ensured the uniform PANI polymer coating on the SPE surface. High-resolution transmission electron microscope (HRTEM) was also employed to investigate the internal structure and polymeric features of PANI. As shown in Fig. 3a, PANI polymeric structure has been revealed as uniformly distributed dark beads with particle size ~0.7–1.1 μm confirming successful polymer formation. The HRTEM-selected area electron diffraction (SAED) pattern (Fig. 3b) exhibits diffuse concentric diffraction rings confirming the polymeric amorphous nature of PANI.

3.6. Electrochemical characterization of SPE/PANI

To ensure that PANI film effectively deposited on SPE, cyclic voltammetry was applied utilizing $[Fe(CN)_6]^{3-}/[Fe(CN)_6]^{4-}$ system as a redox probe to measure the active surface area of the SPE/PANI and bare SPE. As displayed in Fig. S3, SPE/PANI demonstrated higher $[Fe(CN)_6]^{3-}/[Fe(CN)_6]^{4-}$ peak current than bare SPE electrode, indicating PANI's role in increasing the active sensing area via improving the

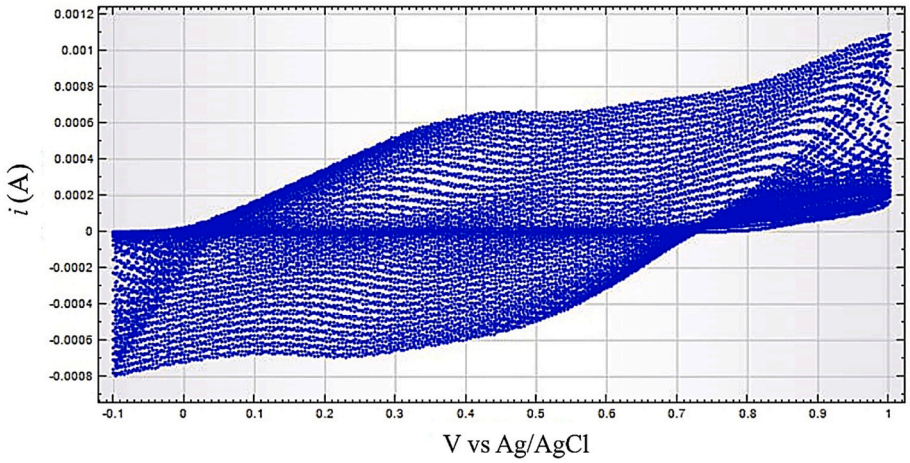

Fig. 1. Electrochemical polymerization of PANI at SPE surface versus Ag/AgCl reference electrode using 0.1 M aniline monomer in 0.1 M H_2SO_4 solution by cyclic voltammetry at −0.1 to 1.0 V vs. Ag/AgCl at scan rate 0.05 V/s for 40 cycles.

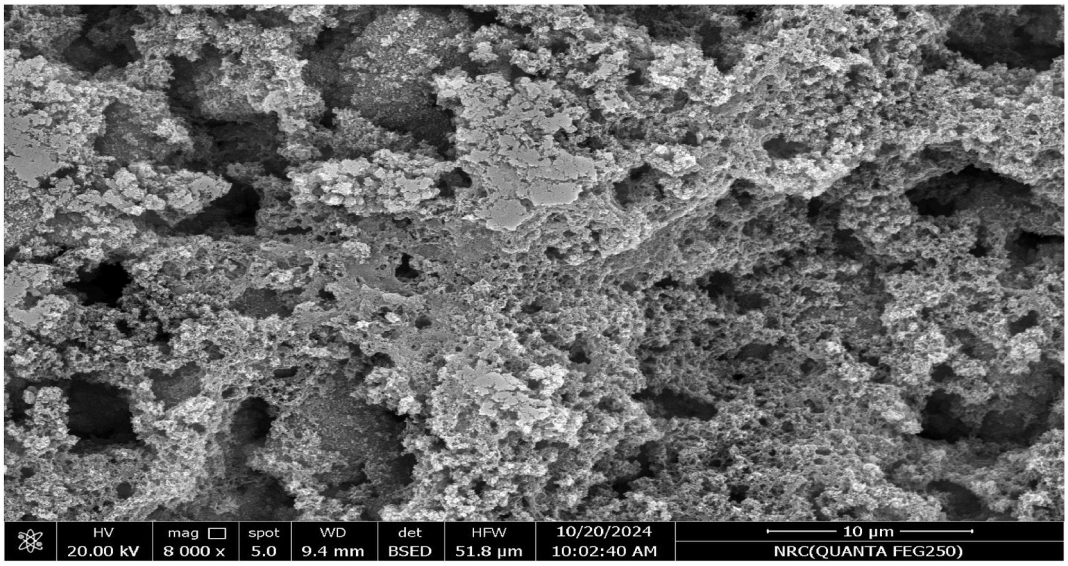

Fig. 2. Scanning electron microscope (SEM) image of modified electrode SPE/PANI.

process of electron transfer. The electroactive surface area (ECSA) was calculated using Randles-Sevcik equation and found to be 0.078 cm^2 for SPE/PANI compared to 0.015 cm^2 for bare SPE.

Moreover, electrochemical impedance spectroscopy (EIS) measurements of the SPE/PANI and bare SPE electrodes were carried out using the $[Fe(CN)_6]^{3-}/[Fe(CN)_6]^{4-}$ redox system. As shown in Fig. S4, SPE/PANI displayed an extremely smaller semicircle compared to bare SPE. The obtained spectra were fitted to Randles equivalent circuit to estimate charge-transfer resistance (Rct) values for both electrodes, Fig. S5. The obtained Rct values were 37.2 Ω and 11.8 kΩ for SPE/PANI and bare SPE, respectively. This significant decrease in SPE/PANI Rct confirms how PANI film effectively deposited on the SPE surface and significantly reduced the charge-transfer resistance through its high conductive nature.

3.7. Screen-printed electrodes' dynamic response time and validation

The dynamic response time is a crucial feature of ion-selective electrodes. It was found that SPE/PANI/CX4 electrode response time is about 3 s, while longer time of about 7 s was required to attain stable potential with SPE/CX4 electrode. The electrochemical performance of the fabricated SPE electrodes; SPE/PANI/CX4 and SPE/CX4, was evaluated according to IUPAC standards [38]. The analytical procedures have been validated in accordance with ICH guidelines [37] using eight different SPEs obtained from two different batches, where four independently fabricated electrodes where used to assess the performance of each electrode, shown in Table 2, where SPE/PANI/CX4 electrode showed a Nernstian slope of 51.481 ± 1.82 over a concentration range (2.50×10^{-6}-1.00×10^{-2} M). SPE/CX4 electrode calibration plot showed Nernstian slope of 52.785 ± 1.06 among concentration range (1.00×10^{-5}-1.00×10^{-2} M). SPE/PANI/CX4 is much more sensitive towards AZE than SPE/CX4 electrode as demonstrated through their limits of quantification and detection. The computed correlation coefficients were 0.9998 and 0.9999 for SPE/PANI/CX4 and SPE/CX4 electrodes, respectively, indicating good linearity over the specified concentration ranges. Potentiometric analysis of three different concentrations of AZE pure standard was used to evaluate the accuracy of measurements obtained by both SPEs. By substituting the obtained responses into the corresponding regression equations, acceptable mean percentage recoveries were computed, confirming the accuracy of both electrodes. The degree of repeatability of the SPEs' measurements was assessed by analyzing three different concentrations of AZE pure standard three

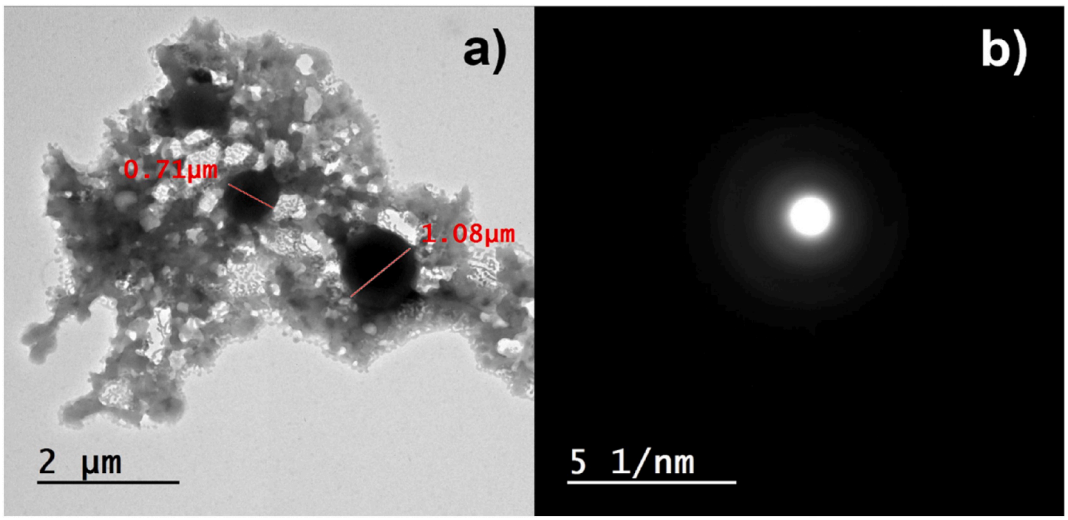

Fig. 3. High-Resolution Transmission Electron Microscope (HRTEM) imaging of PANI showing **a)** polymeric beads, **b)** Selected area electron diffraction (SAED) patterns.

Table 2
Response characteristics of the investigated screen-printed electrodes for the determination of Azelastine HCl.

Parameter	SPE/PANI/CX4	SPE/CX4
Concentration range (M)	2.50×10^{-6}- 1.00×10^{-2}	1.00×10^{-5}- 1.00×10^{-2}
Slope ± SD (mV/decade)[a]	51.481 ± 1.82	52.785 ± 1.06
SE of Slope	0.896	0.536
Intercept ± SD (mV)[a]	540.199 ± 1.60	506.286 ± 1.74
SE of intercept	3.557	1.908
Correlation coefficient (r)	0.9998	0.9999
Working pH range	2-7	2-7
Response time (sec.)	3	7
Stability (weeks)	9	8
Average accuracy[b] ± SD	100.49 ± 0.88	101.42 ± 1.04
Precision		
Repeatability[c] (RSD%)	0.79	1.03
Intermediate precision[d] (RSD %)	1.88	0.91
LOD[e] (M)	1.58×10^{-6}	6.31×10^{-6}

[a] Obtained values for eight independently fabricated electrodes from two different batches (four fabricated for SPE/PANI/CX4 and four fabricated for SPE/CX4 assessment).
[b] Average of three determinations (n = 9).
[c] Repeatability: the intraday precision (n = 9), average of three concentrations repeated three times within the day.
[d] Intermediate precision: the interday precision (n = 9), average of three concentrations repeated three times on three different days.
[e] Limit of Detection (according to IUPAC definition: measured by the intersection of the extrapolated arms of non-responsive and Nernstian calibration segments).

times on the same day. While intermediate precision was evaluated via their analysis on three different days. The obtained %RSD values were less than 2, proving the precision of both electrodes. Calibration plots for the two fabricated SPEs (SPE/PANI/CX4 and SPE/CX4 electrodes) are presented in Fig. 4.

Electrode-to-electrode and inter-batch reproducibility were assessed for SPE/PANI/CX4 and SPE/CX4 using four different SPEs obtained from two different batches for each electrode. SPE/PANI/CX4 yielded an average slope of 51.481 ± 1.82 mV/decade and an average intercept of 540.199 ± 1.60 mV. while SPE/CX4 yielded an average slope of 52.785 ± 1.06 mV/decade and an average intercept of 506.286 ± 1.74 mV. The obtained low SD values demonstrate excellent electrode-to-electrode reproducibility and batch-to-batch consistency. Long-term stability of both electrodes has been confirmed via evaluating the Nernstian slope computed for a single SPE/PANI/CX4 and a single SPE/CX4 electrode. It was found that the SPE/PANI/CX4 retained a Nernstian slope of 50.035 ± 1.39 after 9 weeks, while SPE/CX4 showed a Nernstian slope of 46.021 ± 3.87 after 8 weeks only. The lower SD value for the developed SPE/PANI/CX4 sensor confirms its long-term stability, which could be attributed to the incorporation of the hydrophobic PANI layer at the electrode/ISM interface.

3.8. Water layer and signal drift tests on screen-printed electrodes

Formation of a water layer underneath ion-sensing membrane compromises long-term stability of polyaniline (PANI)-based solid-phase electrodes (SPEs). To address this issue, Pretsch group [60] developed the potentiometric aqueous layer test where the potential drift can be detected upon altering from AZE solution (1.00×10^{-3} M) to a 1.00×10^{-2} M solution of ipratropium bromide (a cationic structurally related compound) then finally replacing ipratropium bromide with the former AZE solution. Fig. 5a reveals that there is barely a water layer formed beneath the ISM in case of SPE/PANI/CX4 electrode. Signal drifting was also examined by documenting *emf* values every 2 min for an hour. The inclusion of polyaniline as a transducer in SPE/PANI/CX4 electrode was the reason behind the high potential stabilization that led to hindering the water layer formation due to its hydrophobic effect and efficient ion-to-electron transduction. SPE/PANI/CX4 electrode revealed a considerable increase in stability accompanied by minimal signal drifting of about 0.6 mV/h compared to SPE/CX4 that displayed 35.5 mV/h (Fig. 5b). SPE/PANI/CX4 was the developed electrode for different applications in this research as it showed higher sensitivity to AZE along with negligible water layer, minimal signal drifting and faster response in comparison to SPE/CX4 electrode. Accordingly, PANI-based screen-printed electrode (SPE/PANI/CX4) was applied for the determination of AZE in its pure powdered form, ophthalmic solution, nasal spray, different spiked biological samples, rabbit aqueous humor, and human plasma.

3.9. Applications

3.9.1. Potentiometric determination of Azelastine HCl in pharmaceutical dosage forms

AZE was quantified in Zelagap® eye drops and Azelast Plus® nasal spray using the optimally developed SPE/PANI/CX4 electrode, without any sample pretreatment. The findings shown in Table 3 ensure that the

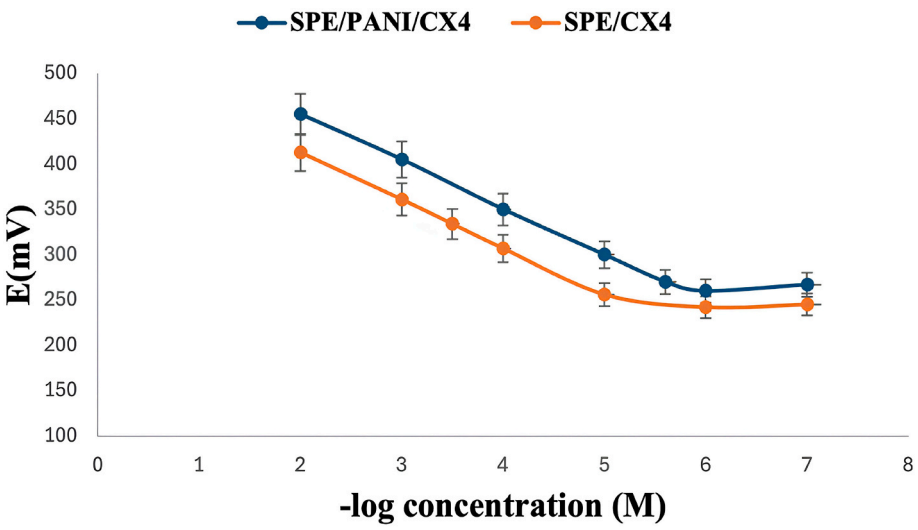

Fig. 4. Profile of the recorded potential in mV versus -Log molar concentration of AZE using SPE/PANI/CX4 and SPE/CX4 sensors.

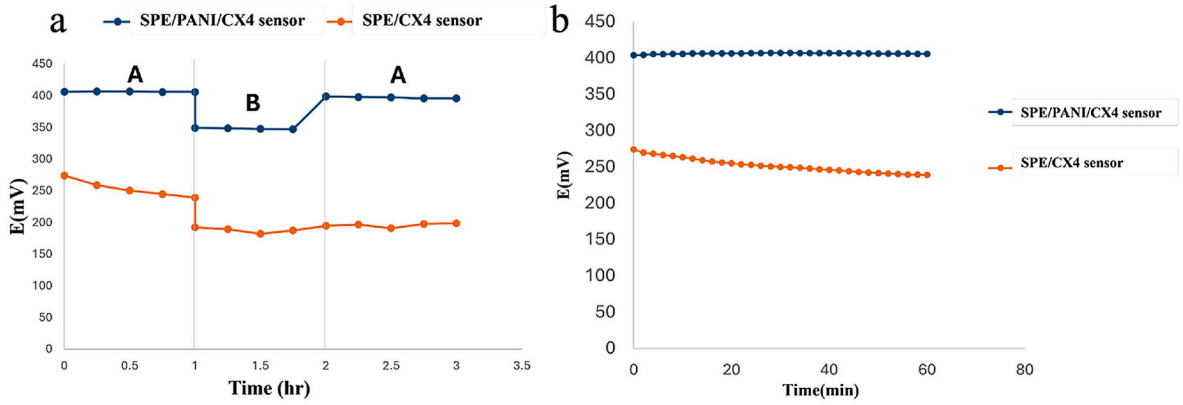

Fig. 5. (a) Water layer test for SPE/PANI/CX4 and SPE/CX4 sensors. Measurements were recorded in $1x10^{-3}$ M AZE (**A**) and $1x10^{-2}$ M ipratropium bromide (**B**). (**b**) Signal drift for SPE/PANI/CX4 and SPE/CX4 sensors. Measurements were recorded in $1.00x10^{-3}$ M AZE.

Table 3
Potentiometric determination of Azelastine HCl in pharmaceutical dosage forms and spiked biological fluids by SPE/PANI/CX4 sensor.

Samples	Concentration (M)	Recovery ± RSD%[a]	Recovery ± RSD%[b]	Student's t-test	F value
Zelagap®	1×10^{-4}	98.25 ± 1.34	99.29 ± 1.60	0.881 (4.303)	1.089 (19)
	1×10^{-5}	101.47 ± 1.53	101.96 ± 1.53		
Azelast Plus®	1×10^{-3}	97.44 ± 1.43	98.33 ± 1.16	0.701 (2.776)	1.485 (19)
	1×10^{-4}	94.33 ± 1.50	99.22 ± 1.13		
Aqueous Humor	1×10^{-3}	95.67 ± 0.11			
	1×10^{-4}	105.56 ± 1.52			
Plasma	1×10^{-3}	100.11 ± 0.96			
	1×10^{-4}	99.92 ± 1.42			

The statistical tests were carried out at $p < 0.05$.
[a] Our developed electrode SPE/PANI/CX4.
[b] Reported method for HPLC/UV determination of Azelastine HCl [55].

developed electrode is highly applicable and can accurately and precisely determine the drug in its dosage forms with no interference either from common interfering ions or from its co-formulated drug, fluticasone propionate.

A published procedure [61] using HPLC/UV was applied effectively to quantify AZE in its dosage forms (Zelagab® and Azelast plus®). Based on statistical evaluation, the reference method and our developed method showed no significant variation, with calculated *t*-test and F-test values falling below the critical tabulated values, as demonstrated in Table 3 [62].

3.9.2. Potentiometric determination of Azelastine HCl in spiked biological samples

The SPE/PANI/CX4 electrode has been used to quantify AZE in spiked rabbit aqueous humor and human plasma samples. AZE can be precisely and accurately determined in the spiked samples with no pretreatment procedures, as shown in Table 3. Regarding C_{max} of AZE in plasma, it varies according to the dose and route of administration [35]. Thus, the measured concentration can be tailored to the desired C_{max} by standard addition or precontraction.

To evaluate the potential matrix effect, two concentration levels

(1×10^{-3} and 1×10^{-4} M) were used for comparing the electrode response obtained in the spiked biological samples (both spiked rabbit aqueous humor and human plasma) with standard solutions of AZE in phosphate buffer at pH 3.0. The calculated matrix effect % for spiked rabbit aqueous humor and human plasma was found to be 99.67% and 99.46%, respectively. The results showed that the electrode response remained minimally affected by components present in the spiked biological samples.

3.10. Electrode's selectivity

The extent of specificity and selectivity of the optimized electrode, SPE/PANI/CX4, towards AZE was examined by applying the separate solution method (SSM) [43]. SPE/PANI/CX4 electrode has shown critical insights into the ability to differentiate between the targeted ion and the different interfering ions. The lower selectivity coefficient value, the less interference and the greater selectivity towards the targeted ion from competing ions, and vice versa. Among the tested ions, it was found that the zinc ions exhibited the lowest selectivity coefficient (0.12) compared to the other ions. Sodium and magnesium's selectivity coefficient values fall in the middle range (0.17 and 0.29, respectively). Both values for potassium and calcium reveal the compromise of the electrode's performance in environments rich in these ions (0.33 and 0.35, respectively).

Among the tested substances were Fluticasone propionate (FLP), AZE co-formulated drug, and AZE possible degradation products, to confirm AZE degradation, AZE IR spectrum shown in (Fig. S6) was attained. Acid degradant (Fig. S7) showed peaks of C═O band of carboxylate group at 1639 cm^{-1} and O-H broad band at 3722 cm^{-1}. While Alkaline degradant (Fig. S8) showed peaks of N-H group at 3438 cm^{-1}, C═C at 1641 cm^{-1}, & absence of carbonyl group. Finally, Oxidative degradation (Fig. S9) showed peaks at 3437 for the O-H & N-H band and the C═O band at 1635 cm^{-1}. Fluticasone propionate & acid degradant exhibited the lowest selectivity coefficients among all the interfering ions tested (0.02 and 0.03, respectively), indicating the electrode's high resistance to acid degradant and FLP interference during targeted ion determination (Table S1).

3.11. Impact of pH and temperature

To find the best conditions for the quantitative measurements of the developed SPE/PANI/CX4 electrode, a pH study was conducted. The potential-pH profile for the developed electrode in 1.00×10^{-3} and 1.00×10^{-4} M AZE solutions was generated and is displayed in Fig. 6a. The electrode showed almost constant potential response over the pH range between 2 and 7. This is believed to be attributed to AZE pKa value (8.88) [52] as the studied drug will be apparently completely ionized, dissociated and detected at pH values 2-7. The potential steadily decreased above pH 7, and at pH 8.5, AZE free base began to precipitate while the potential dropped sharply. This pH decrease may be the result of AZE's non-protonated amino group formation. The stability of measured potential across pH values ranging from 2 to 7 supports our decision to choose the use of phosphate buffer pH 3.0 for the detection of AZE. The effect of temperature on the response of SPE/PANI/CX4 electrode was examined at AZE concentrations range from 2.50×10^{-6} to 1.00×10^{-2} M, and results are illustrated in Fig. 6b. As the temperature rose between 20 and 30°C, there was a modest increase in the electrode's potential without a noticeable impact on the slope or response time. It was revealed that the SPE/PANI/CX4 electrode retains an acceptable degree of thermal stability up to 30°C.

3.12. Comparison against reported and reference methods

The performance of our electrode (SPE/PANI/CX4) has been compared with that of two electrodes reported in the two published papers [25], [27]. One electrode employed graphene nanoplatelets as an ion-to-electron transducer [25], whereas our electrode used PANI as the ion-to-electron transducer. The other electrode incorporated beta-cyclodextrin as a molecular recognition site [27], while the developed sensor incorporated calix[4]arene. The developed electrode (SPE/PANI/CX4) presented in this work demonstrates the most well-rounded analytical characteristics among the reported methods. It provides a broad linear concentration range spanning from 2.50×10^{-6} to 1.00×10^{-2} M, enabling accurate quantification of AZE at both trace and formulation concentrations. The electrode achieves a swift 3-s response time, considerably faster than the two reported methods, indicating efficient ion-to-electron transduction at the solid contact interface. While the detection limit does not represent the lowest value reported, it remains adequate for pharmaceutical and spiked biological applications while circumventing the restricted linearity and fabrication challenges associated with the previously reported methods. The electrode-to-electrode reproducibility of the developed SPE was evaluated using four independently prepared electrodes obtained from different batches, yielding low SD values as mentioned previously under section 3.7, which confirms satisfactory fabrication repeatability and inter-batch consistency. In contrast, the previously reported methods did not provide sufficient information regarding electrode-to-electrode reproducibility evaluation or whether the analytical performance was assessed using a single electrode or multiple independently fabricated electrodes. Regarding fabrication simplicity, the developed solid-contact SPE demonstrates clear practical advantages over the previously reported electrodes. In reported method 1 [25], the fabrication of carbon paste-based electrode involves several operator-dependent steps, including manual paste homogenization, paste packing into the electrode body, adjustment of paraffin content and possible formation of air gaps during packing. In contrast, the developed SPE is fabricated using a standardized industrial screen-printing process, ensuring high fabrication uniformity and

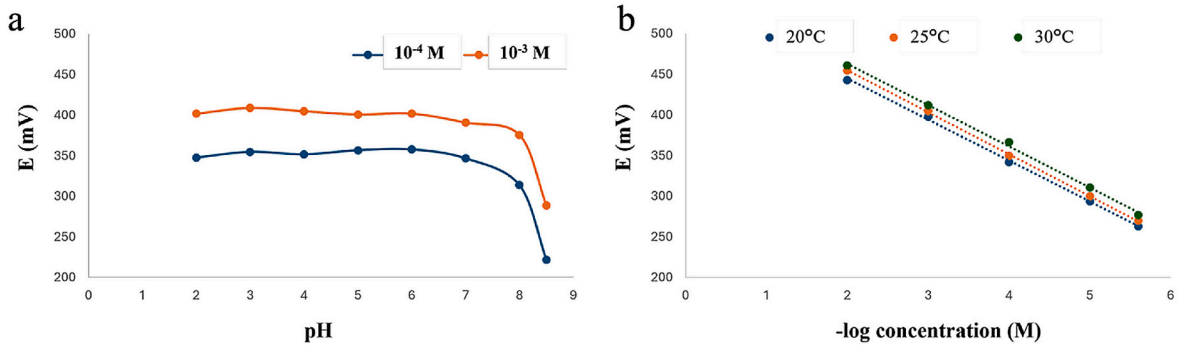

Fig. 6. (a) Effect of pH on the response of SPE/PANI/CX4 sensor [working pH range: 2-7]. **(b)** Effect of temperature (20, 25, 30°C) on the response of SPE/PANI/CX4 sensor.

reproducibility. Furthermore, compared with the conventional liquid-contact electrode described in reported method 2 [27], the developed solid-contact SPE eliminates the need for an internal filling solution, thereby avoiding problems associated with leakage and evaporation of internal solution, while additionally offering advantages of miniaturization, portability, prolonged operational lifetime, and enhanced potential stability. The developed method demonstrated negligible matrix interference in spiked biological samples, with matrix effect values of 99.67% and 99.46% in aqueous humor and plasma, respectively, indicating potential matrix tolerance. In contrast, matrix effect evaluation was not investigated or discussed in the previously reported methods [25,27]. The developed method permits direct analysis of eye drops, nasal spray, aqueous humor, and plasma, highlighting enhanced practical utility and adaptability for authentic sample testing. The comparison parameters were presented in Table S2.

In addition, a statistical analysis was performed to compare results obtained from the developed SPE/PANI/CX4 electrode with those from the official method for pure AZE sample determination [18]. No significant difference was observed in results regarding both precision and accuracy (Table S3).

3.13. Greenness assessment and sustainability profile

Currently, it's challenging to achieve a balance between improving the quality of analytical methods and sustaining a high environmental impact [63]. Therefore, two greenness assessment tools (AGREE(39) and Mo-GAPI(40)) were developed to compare between the eco-friendliness of the developed potentiometric method and two different reported methods [25]' [27].

AGREE is a greenness metric system in the form of a clock-like graph, with a color representation in the middle and an overall score that evaluates twelve principles [39]. While, MoGAPI system generates a cumulative score accompanied by red/green/orange colors, regarding the AGREE assessment tool, the developed method showed a score of 0.83 compared to 0.72 and 0.74 for the first [25] and second [27] reported methods, respectively. According to Mo-GAPI, the developed method is represented by seven aspects on a green color-level scale, including sample preparation, sample transportation, storage, additional sample treatments, human health safety, and safety hazards, where less hazardous and less flammable solvents are used, respectively. Moreover, using potentiometric instrumentation has ensured minimal KWT power usage throughout the process. The full comparison for both assessment tools is shown in Table 4.

Additionally, the method's sustainability was evaluated using the NQS Index [64], which integrates three dimensions — need, quality, and sustainability — providing a comprehensive assessment aligned with UN sustainable development guidelines. The method supported UN-SDGs 3, 4, 5, 7, 9, 12, 13, 14, and 15 (Table S4). As shown in Fig. S10, the method achieved a 100% need score, 86% quality score, and 53% sustainability score, yielding a final index of 80%, confirming its reliability, practicality, and eco-friendliness for AZE determination in pharmaceutical and spiked biological samples.

4. Conclusion

An ion-sensing solid-contact electrode was designed to determine AZE in different spiked biological samples and its pharmaceutical dosage forms (eye drops and nasal sprays). PANI was selected as an interlayer ion-to-electron transducer and showed a superior electrical signal stability with a drift of 0.6 mV/h compared to the other studied electrode with no transducer (35.5 mV/h). Upon performing the water layer test, PANI transducer exhibited a constant potential response, indicating a lack of water between PANI layer and membrane. PANI screen-printed electrode was evaluated based on IUPAC recommendations, showing a slope of 51.481 ± 1.82 mV/decade, a linear range of 2.50×10^{-6} - 1.00×10^{-2} M and LOD of 1.58×10^{-6} M. Upon comprehensive evaluation using recognized greenness assessment tools; MoGAPI and AGREE metrics, the developed analytical method demonstrates a significantly enhanced environmental profile in comparison to the two reported methods. This superiority lies due to alignment with the green analytical chemistry principles, especially downsizing sample sizes and elimination of toxic chemicals. NQS index score was developed to assess sustainability and high-quality performance for analyzing azelastine HCl in both clinical and quality control applications.

Ethical statement

The Committee of Safe Handling and Disposal of Chemicals and Biologicals of Research Ethics at Cairo University's Faculty of Pharmacy granted approval for all experimental procedures conducted in this study (Serial Number: AC (3302)), approved on May 25, 2023.

Table 4
Greenness assessment of the developed potentiometric method for AZE and two reported methods by the Modified GAPI (Mo-GAPI) tool and the Analytical Greenness (AGREE) assessment tool.

Greenness Assessment tools	Developed method	Reported method 1 (2024)[25]	Reported method 2 (2013)[27]
MoGAPI	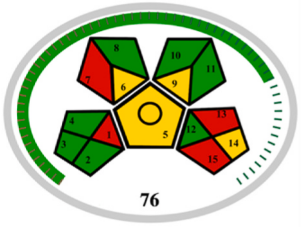	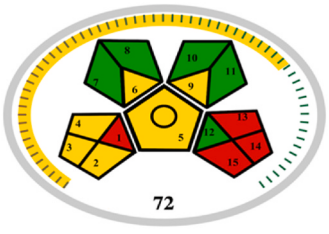	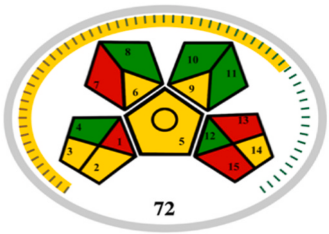
AGREE			

Funding

The author(s) received no financial support for the research, authorship, and/or publication of this article.

CRediT authorship contribution statement

Rawan S. El Meniawy: Conceptualization, Formal analysis, Investigation, Methodology, Validation, Writing – original draft, Writing – review & editing. **Sarah S. Saleh:** Project administration, Supervision, Writing – original draft, Writing – review & editing. **Yasmin Rostom:** Project administration, Supervision, Writing – original draft, Writing – review & editing. **Mona T. Ragab:** Conceptualization, Formal analysis, Investigation, Methodology, Validation, Writing – original draft, Writing – review & editing.

Declaration of competing interest

The authors declare that they have no known competing financial interests or personal relationships that could have appeared to influence the work reported in this paper.

Acknowledgements

The authors would like to thank Dr Essam Eldin A. Osman (Department of Medicinal Chemistry, College of Pharmacy, and Rogel Cancer Center, University of Michigan, USA; Department of Pharmaceutical Chemistry, Faculty of Pharmacy, Cairo University, Egypt) for his assistance in illustrating the mechanism of interaction in AZE–CX4 host–guest complex.

Appendix A. Supplementary data

Supplementary data to this article can be found online at https://doi.org/10.1016/j.talanta.2026.130255.

Data availability

Data will be made available on request.

References

[1] Ö. Isildak, O. Özbek, Application of potentiometric sensors in real samples, Crit. Rev. Anal. Chem. 51 (3) (2021 May 7) 218–231, https://doi.org/10.1080/10408347.2019.1711013. PubMed PMID: 31928212.
[2] S. Yunus, A.M. Jonas, B. Lakard, Potentiometric biosensors [Internet], https://dial.uclouvain.be/pr/boreal/object/boreal:128854, 2013. (Accessed 3 January 2025).
[3] Design of solid-contact ion-selective electrode with graphene transducer layer for the determination of flavoxate hydrochloride in dosage form and in spiked human plasma - mahmoud - 2020 - electroanalysis - wiley online library [Internet], https://analyticalsciencejournals.onlinelibrary.wiley.com/doi/full/10.1002/elan.202060377. (Accessed 19 July 2024).
[4] A.K. Covington, Ion Selective Electrode Method, 1, CRC Press, 2018, p. 266.
[5] L. Gao, Y. Tian, W. Gao, G. Xu, Recent developments and challenges in solid-contact ion-selective electrodes, Sensors 24 (13) (2024 Jan) 13, https://doi.org/10.3390/s24134289.
[6] D.L. Glasco, N.H.B. Ho, A.M. Mamaril, J.G. Bell, 3D printed ion-selective membranes and their translation into point-of-care sensors, Anal. Chem. 93 (48) (2021 Dec 7) 15826–15831, https://doi.org/10.1021/acs.analchem.1c03762.
[7] H.E. Zittel, F.J. Miller, ACS Publications [research-article] [Internet]. American Chemical Society, A glassy-carbon electrode for voltammetry, Located at: world. (2002), https://doi.org/10.1021/ac60221a006. Available from: https://pubs.acs.org/doi/pdf/10.1021/ac60221a006. (Accessed 6 August 2024).
[8] H.J. James, G. Carmack, H. Freiser, ACS Publications [research-article] [Internet]. American Chemical Society, Coated wire ion-selective electrodes, Located at: world. Available from: (2002), https://doi.org/10.1021/ac60312a046. https://pubs.acs.org/doi/pdf/10.1021/ac60312a046. (Accessed 7 August 2024).
[9] Copper and nickel microsensors produced by selective laser reductive sintering for non-enzymatic glucose detection, Materials 14 (10) (2021 May 12) 2493, https://doi.org/10.3390/MA14102493.
[10] R.R. Suresh, M. Lakshmanakumar, J.B.B. Arockia Jayalatha, K.S. Rajan, S. Sethuraman, U.M. Krishnan, et al., Fabrication of screen-printed electrodes: opportunities and challenges, J. Mater. Sci. 56 (15) (2021 May) 8951–9006, https://doi.org/10.1007/s10853-020-05499-1.
[11] E. Jaworska, W. Lewandowski, J. Mieczkowski, K. Maksymiuk, A. Michalska, Simple and disposable potentiometric sensors based on graphene or multi-walled carbon nanotubes – carbon–plastic potentiometric sensors, Analyst 138 (8) (2013 Mar 18) 2363–2371, https://doi.org/10.1039/C3AN36741J.
[12] R. Hernández, J. Riu, J. Bobacka, C. Vallés, P. Jiménez, A.M. Benito, et al., Reduced graphene oxide films as solid transducers in potentiometric all-solid-state ion-selective electrodes, J. Phys. Chem. C 116 (42) (2012 Oct 25) 22570–22578, https://doi.org/10.1021/jp306234u.
[13] F. Li, J. Ye, M. Zhou, S. Gan, Q. Zhang, D. Han, et al., All-solid-state potassium-selective electrode using graphene as the solid contact, Analyst 137 (3) (2012 Jan 10) 618–623, https://doi.org/10.1039/C1AN15705A.
[14] A.H. Kamel, A.E.G.E. Amr, N.S. Abdalla, M. El-Naggar, M.A. Al-Omar, H. M. Alkahtani, et al., Novel solid-state potentiometric sensors using polyaniline (PANI) as A solid-contact transducer for flucarbazone herbicide assessment, Polymers 11 (11) (2019 Nov) 11, https://doi.org/10.3390/polym11111796.
[15] G. Hussein O, A. Ahmed D, M. Abdelkawy, R. Rezk M, M. Mahmoud A, Y. Rostom, Novel solid-contact ion-selective electrode based on a polyaniline transducer layer for determination of alcaftadine in biological fluid, RSC Adv. 13 (11) (2023) 7645–7655, https://doi.org/10.1039/D3RA00597F.
[16] A.M. Mahmoud, M.K. Abd El-Rahman, M.R. Elghobashy, M.R. Rezk, Carbon nanotubes versus polyaniline nanoparticles; which transducer offers more opportunities for designing a stable solid contact ion-selective electrode, J. Electroanal. Chem. 755 (2015 Oct) 122–126, https://doi.org/10.1016/j.jelechem.2015.07.045.
[17] I.A. Pechenkina, K.N. Mikhelson, Materials for the ionophore-based membranes for ion-selective electrodes: problems and achievements (review paper), Russ. J. Electrochem. 51 (2) (2015 Feb) 93–102, https://doi.org/10.1134/S1023193515020111.
[18] British pharmacopeia, in: The British Pharmacopoeia. London: Stationary Office, 2020, pp. I236–I237.
[19] J.M. Horbal, J.A. Bernstein, Azelastine HCl: a review of the old and new formulations, Clin. Med. Insights Ther. 2 (2010 Jan), https://doi.org/10.4137/CMT.S3865.
[20] H.A. Merey, S.S. El-Mosallamy, N.Y. Hassan, B.A. El-Zeany, Simultaneous determination of fluticasone propionate and Azelastine hydrochloride in the presence of pharmaceutical dosage form additives, Spectrochim. Acta Mol. Biomol. Spectrosc. 160 (2016 May 5) 50–57, https://doi.org/10.1016/j.saa.2016.02.010. PubMed PMID: 26921606.
[21] M. Hassouna, M. Abdelrahman, M. Abdelfatah, Determination of azelastine hydrochloride and benzalkonium chloride in their ophthalmic solution by different spectrophotometric methods, World J Appl Chem. 2 (2017 Mar 10) 48–56, https://doi.org/10.11648/j.wjac.20170202.12.
[22] N.N. Salama, S.A. Abdel-Razeq, S. Abdel-Atty, N. El-Kosy, Spectrophotometric determination and thermodynamic studies of the charge transfer complexes of azelastine-HCl, Bull. Fac. Pharm. Cairo Univ. 49 (1) (2011 Jun 1) 13–18, https://doi.org/10.1016/j.bfopcu.2011.07.003.
[23] W.N. Abd-AlGhafar, F.A. Aly, Z.A. Sheribah, S. Saad, Synchronous fluorescence as a green and selective method for the simultaneous determination of cetirizine and azelastine in aqueous humor, J. Fluoresc. 32 (3) (2022 May 1) 1199–1210, https://doi.org/10.1007/s10895-022-02913-6.
[24] A.A. El-Masry, M.E.A. Hammouda, D.R. El-Wasseef, S.M. El-Ashry, Validated sensitive spectrofluorimetric method for determination of antihistaminic drug azelastine HCl in pure form and in pharmaceutical dosage forms: application to stability study, Lumin J Biol Chem Lumin. 32 (2) (2017 Mar) 177–181, https://doi.org/10.1002/bio.3164. PubMed PMID: 27279096.
[25] M.H. Mohamed, N.N. Mikawy, N. Magdy, A.M. Elkosasy, Ion selective electrodes with ionophore-doped sensing membranes and graphene nanoplatelets for determination of azelastine HCl in nasal spray and plasma, Arch Pharm Sci Ain Shams Univ 8 (2) (2024 Dec 1) 313–327, https://doi.org/10.21608/aps.2024.293159.1174.
[26] S.A. Abdel-Razeq, M.M. Foaud, N.N. Salama, S. Abdel-Atty, N. El-Kosy, Voltammetric determination of Azelastine-HCl and emedastine dirumarate in micellar solution at glassy carbon and carbon paste electrodes [Internet], https://dk.upce.cz//handle/10195/42515, 2011. (Accessed 1 July 2024).
[27] M.R. Elghobashy, O.M. Badran, M.Y. Salem, K.M. Kelani, Application of membrane selective electrodes for the determination of azelastine hydrochloride in the presence of its alkaline degradant in eye drops and plasma, Anal. Bioanal. Electrochem. 5 (3) (2013 Jun) 325–340. Located at: world.
[28] G. Singh, S. Rani, Determination of azelastine in different samples by poly (vinyl chloride) based membrane electrode, Asian J Pharm Anal 3 (2013) 37–41.
[29] W.N. Abd-AlGhafar, F.A. Aly, Z.A. Sheribah, S. Saad, Factorial design-assisted reverse phase HPLC–UV approach for the concurrent estimation of cetirizine and azelastine in aqueous humor, Sci. Rep. 12 (1) (2022 Dec 27) 22435, https://doi.org/10.1038/s41598-022-26774-y.
[30] R.N. El-Shaheny, K. Yamada, Stability study of the antihistamine drug azelastine HCl along with a kinetic investigation and the identification of new degradation products, Anal Sci Int J Jpn Soc Anal Chem. 30 (6) (2014) 691–697, https://doi.org/10.2116/analsci.30.691. PubMed PMID: 24919676.
[31] J. Pivonka, F.H. Segelman, C.A. Hartman, W.E. Segl, N. Kucharczyk, R.D. Sofia, Determination of azelastine and desmethylazelastine in human plasma by high-performance liquid chromatography, J Chromatogr B Biomed Sci App 420 (1987 Jan 1) 89–98, https://doi.org/10.1016/0378-4347(87)80158-5.
[32] N.N. Salama, S.A. Abdel-Razeq, S. Abdel-Atty, N. El-Kosy, Development and validation of densitometry TLC stability indicating method for quantitative

determination of azelastine hydrochloride and emedastine difumarate in their drug products, J. Pharm. Res. Int. (2014) 79–92, https://doi.org/10.9734/BJPR/2014/3693.
[33] U. Heinemann, G. Blaschke, N. Knebel, Simultaneous enantioselective separation of azelastine and three of its metabolites for the investigation of the enantiomeric metabolism in rats: I. Liquid chromatography–ionspray tandem mass spectrometry and electrokinetic capillary chromatography, J. Chromatogr. B 793 (2) (2003 Aug 15) 389–404, https://doi.org/10.1016/S1570-0232(03)00357-X.
[34] Y.S. Park, S.H. Kim, Y.J. Kim, S.C. Yang, M.H. Lee, L.M. Shaw, et al., Determination of azelastine in human plasma by validated liquid chromatography coupled to tandom mass spectrometry (LC-ESI/MS/MS) for the clinical studies, Int J Biomed Sci IJBS 6 (2) (2010 Jun) 120–127. PubMed PMID: 23675185; PubMed Central PMCID: PMC3614744.
[35] S.C. Sweetman, C. Martindale, The Complete Drug Reference, 1, Pharmaceutical press, London, 2009.
[36] Y. Rostom, O.G. Hussein, A.M. Mahmoud, M. Abdelkawy, M.R. Rezk, D.A. Ahmed, Novel carbon nanotubes/gold nanoparticles modified carbon paste electrochemical sensor for antazoline determination in aqueous humor, J. Electrochem. Soc. 171 (3) (2024) 037510.
[37] Y. Umezawa, et al., International conference on harmonization (ICH), Q2B: validation of analytical procedures methodology, 62, US FDA Federal Register 1997 72 (10) (2000) 1851–2082, 72.
[38] R. Iupac, I.R. Iupac, Analytical chemistry division, commission on analytical nomenclature, Pure Appl. Chem. 72 (2000) 1851–2082.
[39] F. Pena-Pereira, W. Wojnowski, M. Tobiszewski, AGREE—Analytical GREEnness metric approach and software, Anal. Chem. 92 (14) (2020 Jul 21) 10076–10082, https://doi.org/10.1021/acs.analchem.0c01887.
[40] F.R. Mansour, K.M. Omer, J. Płotka-Wasylka, A total scoring system and software for complex modified GAPI (ComplexMoGAPI) application in the assessment of method greenness, Green Anal Chem 10 (2024 Sep 1) 100126, https://doi.org/10.1016/j.greeac.2024.100126.
[41] F.J. Feliciano, O.C. Monteiro, New nanocomposite materials by incorporation of nanocrystalline TiO2 particles into polyaniline conductive films, J. Mater. Sci. Technol. 30 (5) (2014) 449–454.
[42] S.S. Soliman, A.M. Mahmoud, A.A. Mouhamed, O.G. Hussein, Electrochemical sensor modified with heterostructure of graphitic carbon nitride/gold nanoparticles for non-invasive uric acid detection in saliva, Sens. Biosens. Res. (2025) 100881.
[43] Tsu Sheng Ma Ts, S. Hassan, Organic Analysis Using ion-selective Electrodes, Blackwell Science, 1982.
[44] B. Meibohm, H. Möllmann, M. Wagner, G. Hochhaus, A. Möllmann, H. Derendorf, The clinical pharmacology of fluticasone propionate, Rev. Contemp. Pharmacother. 8 (1998 Jan 1) 535, 8, 535-549 (1998).
[45] A.M. El-Kosasy, M.A. Shehata, N.Y. Hassan, A.S. Fayed, B.A. El-Zeany, Membrane electrodes for the determination of glutathione, Talanta 66 (3) (2005 Apr 30) 746–754, https://doi.org/10.1016/j.talanta.2004.12.027.
[46] F.M. Abdel-Haleem, M. Saad, A. Barhoum, M. Bechelany, M.S. Rizk, PVC membrane, coated-wire, and carbon-paste ion-selective electrodes for potentiometric determination of galantamine hydrobromide in physiological fluids, Mater Sci Eng C 89 (2018 Aug) 140–148, https://doi.org/10.1016/j.msec.2018.04.001.
[47] M. Heba, N. Ramadan, M. El-Laithy, Polymeric matrix membrane sensors for stability-indicating potentiometric determination of oxybutynin hydrochloride and flavoxate hydrochloride urogenital system drugs, J. AOAC Int. 91 (6) (2008 Nov 1) 1318–1330, https://doi.org/10.1093/jaoac/91.6.1318.
[48] H.M. Abu Shawish, A.M. Khedr, K.I. Abed-Almonem, M. Gaber, A comparative study of solid and liquid inner contact benzalkonium chloride ion-selective electrode membranes, Talanta 101 (2012 Nov 15) 211–219, https://doi.org/10.1016/j.talanta.2012.09.005.
[49] M.E. Henawee, A.R. Derar, H. Saleh, A. Attia, E. Hussien, All-solid-state disposable polymeric ion selective electrode for determination of milnacipran in pharmaceutical dosage form, IEEE Sens. J. 19 (2019) 11746–11752, https://doi.org/10.1109/JSEN.2019.2940196.
[50] P. Bühlmann, E. Pretsch, E. Bakker, Carrier-based ion-selective electrodes and bulk optodes. 2. Ionophores for potentiometric and optical sensors, Chem Rev. 98 (4) (1998 Jun 1) 1593–1688, https://doi.org/10.1021/cr970113+.
[51] M.P.S. Mousavi, M.K. Abd El-Rahman, A.M. Mahmoud, R.M. Abdelsalam, P. Bühlmann, In situ sensing of the Neurotransmitter Acetylcholine in a dynamic range of 1 nM to 1 mM, ACS Sens. 3 (12) (2018 Dec 28) 2581–2589, https://doi.org/10.1021/acssensors.8b00950.
[52] A. Reda, H. Saleh, E. Bahgat, M. Fawzy, Analytical methods for determination of azelastine hydrochloride and fluticasone propionate in different matrices: a mini review, ERU Res J 0 (0) (2024 Apr 25), https://doi.org/10.21608/erurj.2024.235608.1075, 0–0.
[53] C. Mihali, N. Vaum, Use of plasticizers for electrochemical sensors, Recent Adv Plast. 125 (2012).
[54] A. Ceresa, E. Pretsch, Determination of formal complex formation constants of various Pb2+ ionophores in the sensor membrane phase, Anal. Chim. Acta 395 (1) (1999 Aug 16) 41–52, https://doi.org/10.1016/S0003-2670(99)00311-6.
[55] Z. Han, K.Y. Wang, Y. Guo, Z.H. Wang, R.R. Liang, Y. Yang, et al., Multiple host–guest interactions in metal–organic frameworks constructed by inverted Calix [4]arenes, J. Am. Chem. Soc. 147 (29) (2025 Jul 23) 25162–25166, https://doi.org/10.1021/jacs.5c08164.
[56] E.S. Español, M.M. Villamil, Calixarenes: generalities and their role in improving the solubility, biocompatibility, stability, bioavailability, detection, and transport of biomolecules, Biomolecules 9 (3) (2019 Mar) 90, https://doi.org/10.3390/biom9030090.
[57] C.H. Yang, T.C. Wen, Polyaniline derivative with external and internal doping via electrochemical copolymerization of aniline and 2,5-Diaminobenzenesulfonic acid on IrO2 - coated titanium electrode, J. Electrochem. Soc. 141 (10) (1994 Oct 1) 2624, https://doi.org/10.1149/1.2059144.
[58] K. Naoi, K ichi Kawase, M. Mori, M. Komiyama, Electrochemistry of Poly(2,2′-dithiodianiline): a new class of high energy conducting polymer interconnected with S−S bonds, J. Electrochem. Soc. 144 (6) (1997 Jun 1) L173, https://doi.org/10.1149/1.1837715.
[59] R.A. Gaber, N.Y. Hassan, N.K. Ramadan, M.T. Ragab, Solid-contact ion-selective sensor for the direct determination of procyclidine HCl and application of in-line dissolution profiling of its tablets, Electroanalysis 36 (8) (2024) e202300363, https://doi.org/10.1002/elan.202300363.
[60] M. Parrilla, M. Cuartero, G.A. Crespo, Wearable potentiometric ion sensors, TrAC Trends Anal Chem 110 (2019 Jan 1) 303–320, https://doi.org/10.1016/j.trac.2018.11.024.
[61] S. Patel, P. Ty, STABILITY-INDICATING high-performance liquid chromatography method for determination of antihistamine drug azelastine, Asian J Pharm Clin Res 11 (8) (2018 Aug 7) 248, https://doi.org/10.22159/ajpcr.2018.v11i8.25506.
[62] J.N. Miller, J.C. Miller, Statistics and Chemometrics for Analytical Chemistry, sixth ed., Pearson Education Ltd, Harlow. - References - Scientific Research Publishing, 2010 [Internet]. https://www.scirp.org/reference/referencespapers?referenceid=3657727&utm_source=chatgpt.com. (Accessed 19 April 2026).
[63] S.S. Saleh, R.H. Obaydo, M.A. El Hamd, Y. Rostom, D. Mohamed, H.M. Lotfy, Guidelines for accurate application of green and white analytical concepts: merits versus demerits with insights of significant milestones of assessment tools applied for antiviral drugs, Microchem. J. 199 (2024 Apr 1) 109917, https://doi.org/10.1016/j.microc.2024.109917.
[64] K. Kiwfo, S. Suteerapataranon, I.D. McKelvie, P. Meng Woi, S.D. Kolev, C. Saenjum, et al., A new need, quality, and sustainability (NQS) index for evaluating chemical analysis procedures using natural reagents, Microchem. J. 193 (2023 Oct 1) 109026, https://doi.org/10.1016/j.microc.2023.109026.